6.6 THE SOUTHERN PLAINS EXPERIMENT IN CLOUD SEEDING OF THUNDERSTORMS FOR RAINFALL AUGMENTATION (SPECTRA) PROJECT: OPERATIONAL TOOLS USED TOWARDS VERIFYING GLACIOGENIC AND HYGROSCOPIC SEEDING CONCEPTUAL MODELS, CASE STUDIES AND PRELIMINARY RESULTS.

Duncan Axisa
Southern Ogallala Aquifer Rainfall (SOAR) program, Plains, Texas

Daniel Rosenfeld
The Hebrew University of Jerusalem, Jerusalem, Israel

Joshua L. Santarpia
Texas A&M University, College Station, Texas

William L. Woodley
Woodley Weather Consultants, Littleton, Colorado

Don R. Collins
Texas A&M University, College Station, Texas

1. INTRODUCTION

The Southern Plains Experiment in Cloud Seeding of Thunderstorms for Rainfall Augmentation (SPECTRA) Project was designed to study convective clouds in the southern plains, specifically areas in Texas, southeastern New Mexico and Oklahoma where advertent and/or inadvertent weather modification occurs. The objectives of the SPECTRA project are to document microphysical signatures produced by glaciogenic base seeding, document the Cloud Condensation Nuclei (CCN) distribution and their effect on the cloud Drop Size Distribution (DSD), test hygroscopic seeding using milled salt and finally, conduct model simulations of seeded and non-seeded clouds. In order to achieve these objectives, a field program was designed starting initially with Phase 1 which focused on the collection of CCN number concentrations and CCN size distributions at cloud base and measurement of the DSD spectra of convective clouds at various levels from cloud base to cloud top.

A new Texas based cloud physics aircraft was equipped specifically as part of this project. The Southern Ogallala Aquifer Rainfall (SOAR) program Cheyenne II was equipped with instrumentation that has the capability of measuring in-situ microphysical properties of clouds and their thermodynamic environment.

For adequate sampling of particles in and around clouds, the research aircraft has the capability of measuring the size distribution of aerosols ranging from 0.1 µm to 3µm and hydrometeors from 2 µm to 1.55 mm in diameter. This dynamic range is achieved by the permanent platform of the SOAR research aircraft. This paper details the SOAR research aircraft instrumentation platform and description of data collected during the SPECTRA project by referring to two case study days, the 14th of August 2004 and the 23rd of August 2004.

Corresponding author address: Duncan Axisa, SOAR program, PO Box 130, Plains, TX 79355.
E-mail: soar@sandylandwater.com

2. DEPLOYMENT OF THE SOAR RESEARCH AIRCRAFT

2.1 The use of FX-Net during SPECTRA

During the SPECTRA project, suites of data sources were used to ascertain the location of convective initiation and ensuing propagation. A key component of the forecast decision making process was the FX-Net system developed by the Forecast Systems Laboratory (FSL). FX-Net is a meteorological PC workstation that provides access to the basic display capability of an Advanced Weather Interactive Processing System (AWIPS) workstation via the Internet. One of the most important factors in determining convective initiation is finding mesoscale features that might create enough lift for thunderstorms to develop. Using FX-Net, the SPECTRA forecaster was able to visualize boundaries and convergent wind fields that might initiate storms by looking at model output data at high resolutions and then overlaying this with actual data, such as radar imagery or upper level winds. In addition, model instability fields could be plotted at high resolution and overlayed onto radar imagery giving an impression for which convective complexes might be encountering the most instability. 850mb and 700mb NGM parcel trajectories were used to determine the trajectories of aerosols. FX-Net was also used in SPECTRA weather briefings as the presentation tools were very useful in pulling weather products up quickly for discussion.

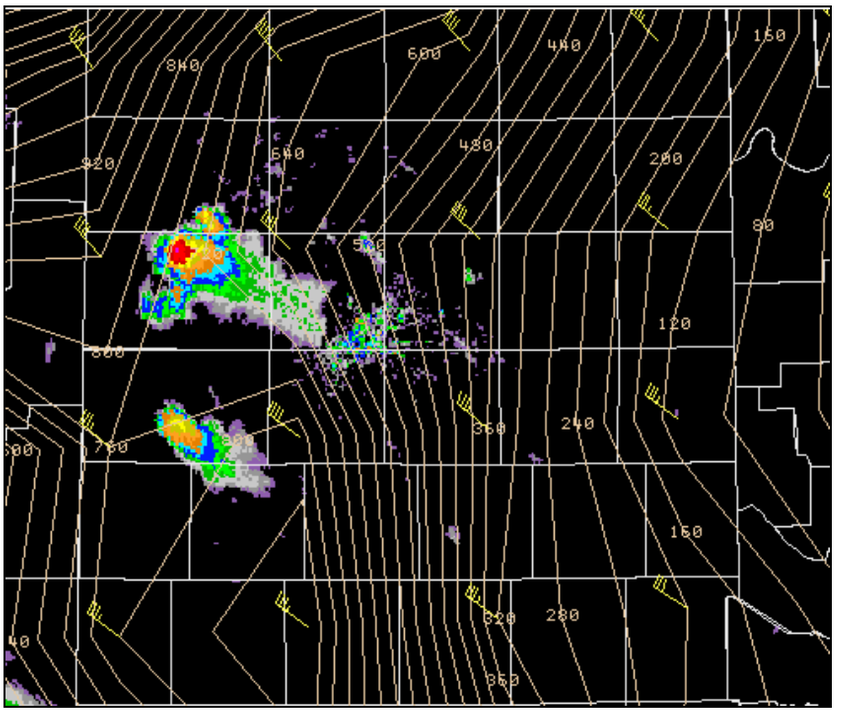

Figure 1: FX-Net overlays Eta 0-6km Bulk shear vectors and surface buoyancy 15 Aug 04 00:00Z forecast fields onto the Amarillo composite reflectivity 14 Aug 04 22:49Z.

2.2 Texas regional mosaic WSR-88D Level II data

Another useful tool during SPECTRA was the Texas regional mosaic IRaDS (Integrated Radar Data Services) WSR-88D Level II data. These National Weather Service (NWS) WSR-88D sites cover the Texas weather modification programs' target areas. NEXRAD data is run through Thunderstorm Identification, Tracking, Analysis, and Nowcasting (TITAN) as a graphic user interface, enabling the radar meteorologist to examine the three-dimensional structure of echoing clouds in real time. Individual echoes and groups of echoes can be tracked and their development and motion projected in time. Airborne Data Acquisition and Telemetry System onboard the research aircraft allows the radar meteorologist at each seeding target to track the SOAR research aircraft on TITAN and vector the aircraft to regions of enhanced convection within the Ultra High Frequency (UHF) range of the telemetry system. During the field measurement program (phase 1), the SOAR research aircraft was mostly deployed in targets of existing weather modification programs in Texas. This allowed the crew on the research aircraft to communicate with the project meteorologist at each weather modification site in Texas to obtain supplemental radar information to that available onboard the research aircraft. The aircraft flight tracks can also be used to associate the cloud physics in situ data with the cloud radar echoes.

3. THE CLOUD PHYSICS PLATFORM ON THE SOAR CHEYENNE II DURING SPECTRA

3.1 The SOAR research aircraft

The SOAR research aircraft is a Piper PA-31T Cheyenne II cloud penetrating aircraft. The Cheyenne has research airspeed of 85 ms^{-1} to 95 ms^{-1} and when performing climbing penetrations, the research ceiling is 25000 feet. The research aircraft has the capability of measuring the size distribution of aerosols ranging from 0.1 µm to 3 µm and hydrometeors from 2 µm to 1.55 mm in diameter. The platform of the SOAR research aircraft during SPECTRA consisted of the Particle Measuring Systems' (PMS) Passive Cavity Aerosol Spectrometer Probe (PCASP SPP-200), the Droplet Measurement Technologies (DMT) Cloud Droplet Probe (CDP) and the DMT Cloud Imaging Probe (CIP). This range gives the scientists a spectrum of measurements in the temporarily suspended aerosol range and in the cloud hydrometeor range. In addition, inferences on the cloud composition and the particles that act as CCN can be achieved by DMT's airborne CCN counter. The SOAR research aircraft was also equipped with Texas A&M University's aircraft-based high flow rate Differential Mobility Analyzer (DMA)/Tandem Differential Mobility Analyzer (TDMA) for sequential measurement of the hygroscopic growth of particles and measurements of the aerosol concentrations as a function of size to determine the critical supersaturation spectrum of aerosols.

3.2 Basic instrument package for the SOAR research aircraft during SPECTRA

VARIABLE	INSTRUMENT	RANGE	ACCURACY	RESOLUTION	FREQUENCY
Air temperature (reverse flow)	0.038" DIA. Bead Thermistor	-30°C to +50°C	0.05°C/0.3°C incl DHC	0.01°C	< 1 s TC
Relative humidity (reverse flow)	Thermoset Polymer RH Sensor	0 to 100% RH	2% RH	0.1% RH	5 s TC @ 20°C
Barometric pressure	MEMS Pressure Sensor	0 to 110000 Pa	100 Pa	10 Pa	20 Hz
u wind component (+ North)	Extended Kalman Filter (EKF)		0.50 m/s @ 75 m/s TAS	0.01 m/s	5 Hz
v wind component (+ East)	Extended Kalman Filter (EKF)		0.50 m/s @ 75 m/s TAS	0.01 m/s	5 Hz
w wind component (+ Down)	Extended Kalman Filter (EKF)		0.50 m/s @ 75 m/s TAS	0.01 m/s	5 Hz
Position (Latitude/Longitude)	WAAS DGPS		2 m (2 σ)	< 1 m	5 Hz
Altitude	WAAS DGPS	-300 to 18000 m	5 m (2 σ)	< 1 m	5 Hz
Geometric Altitude	King KRA 405 Radar Altimeter	0 to 2000 ft	3% < 500 ft 5% > 500 ft	0.48 ft (0.15 m)	
Roll Attitude (ϕ)	MEMS IMU/GPS/EKF	-60 to +60°	0.1°	0.01°	5 Hz
Pitch Attitude (θ)	MEMS IMU/GPS/EKF	-60 to +60°	0.2°	0.01°	5 Hz
Yaw Attitude (ψ)/ Heading	MEMS IMU/GPS/EKF	0 to 360°	0.1°	0.01°	5 Hz
Angle of attack (α)	MEMS Pressure Sensor	-15 to +15°	0.03° @ 150 m/s	0.001° @ 150 m/s	20 Hz
Side-slip (β)	MEMS Pressure Sensor	-15 to +15°	0.03° @ 150 m/s	0.001° @ 150 m/s	20 Hz
True Air Speed	MEMS Pressure Sensor	0 to 150 m/s	0.1 m/s	0.01 m/s	20 Hz
Video record	Sony DCR-DVD 201				
Logging, telemetry & event markers	ESD DTS (GPS)				1 Hz
Cloud droplet spectra	DMT CDP	2 to 50 µm		1 to 2 µm, 30 bins	1 Hz
Cloud particle spectra	DMT CIP	25 to 1550 µm		25 µm, 62 bins	1 Hz
Cloud particle image	DMT CIP	25 to 1550 µm		25 µm	
Liquid water content	DMT LWC-100	0 to 3 g/m^3	0.05 g/m^3	0.01 g/m^3	1 Hz
	CDP calculated	> 3 g/m^3			1 Hz
Aerosol spectrometer	PMS PCASP SPP-200	0.1 to 3 µm		0.02 µm, 30 bins	1 Hz
Aerosol properties	TAMU DMA/TDMA	see text			1 Hz
CCN	DMT CCN counter	0.5 to 10 µm 0.1 to 1.2 % SS	see text	0.5 µm, 20 bins	1 Hz

Table 1: Summary of parameters and measuring devices used on the SOAR Cheyenne II.

Figure 2a: The SOAR Cheyenne II cloud physics aircraft.

Figure 2b: The DMT CIP probe and the DMT CDP probe.

Figure 2c: Aventech Research AIMMS-20 and PMS PCASP.

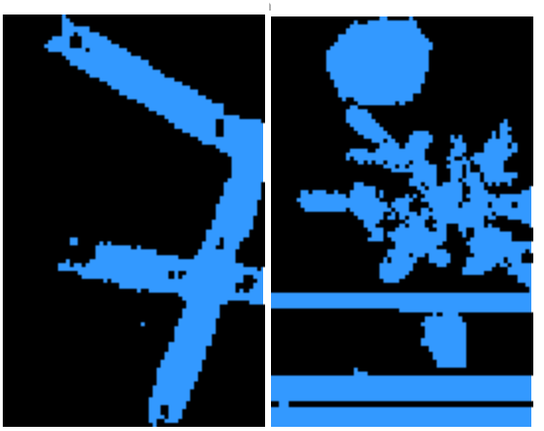

Figure 2d: Needles, spherical graupel and a dendritic crystal imaged by the CIP probe east of Midland TX in a cold front on 25 Sep 2004.

3.3 The DMT CCN counter

The DMT CCN counter samples aerosols from outside the aircraft to measure their capability to act as cloud condensation nuclei. The air sample enters the top center of the 50 cm long vertical cylindrical column and as the air sample flows down through the chamber, CCN activate in response to the exposed supersaturation and grow to droplets. An optical particle counter at the base or outlet of the chamber detects all particles with diameters larger than 0.5µm. The unit operates at a single supersaturation. The supersaturation can be varied between 0.1% and 1.2%. Approximately 30 seconds are required for a shift from one supersaturation to another, although operation in the field shows that shifting from a high supersaturation (1.0%) to a low supersaturation (0.1%) may take more than a minute since the column's three temperature controllers are more efficient at warming than at cooling. The data output is distributed in 20 bins of resolution over the sizing range of 0.75 µm to 10 µm. At a sample flow rate of 60 vccm, 6000 particles per cubic centimeter can be counted with a maximum of a 10% coincidence. During SPECTRA, the CCN counter was mostly operated at supersaturation steps of 0.1, 0.25, 0.5 and 1.0%. Particles that exit the base of the column and are in bin 1 through bin 20 comprise the measured CCN concentration.

3.4 The Texas A&M University DMA/TDMA

Texas A&M University owns and operates a DMA/TDMA system that measures aerosol size distributions and size resolved hygroscopic growth. A DMA uses an electric field to separate particles within a narrow range of electrical mobility. If the voltage is fixed, a monodisperse aerosol may be separated from a polydisperse population. If the voltage is varied, the distribution of aerosol particles may be obtained. Since the electrical mobility is related to the diameter of the particle and the amount of charge on the particle, aerosols are neutralized prior to classification so that the

relationship between size and electrical mobility is unique. The TDMA uses two DMAs in tandem to measure the hygroscopic growth of particles exposed to a controlled relative humidity (RH). The first DMA is used to select particles of a single dry size, which are then exposed to a controlled RH. The distribution of humidified particles is then scanned by the second DMA to determine the fraction of those particles that grew in response to the change in RH. The particles containing hygroscopic material will grow according to the amount and type of hygroscopic material they contain, and those that are non-hygroscopic will remain the same size (Gasparini et al., 2004). During the SPECTRA project, size distributions of the ambient aerosol from 0.010µm to 0.500µm and hygroscopic growth distribution at 85% RH were measured for particles with dry sizes from 0.013µm to 0.300µm.

4. SPECTRA CASE STUDIES: MESOSCALE CONDITIONS, CLOUD MICROPHYSICAL PROPERTIES AND AEROSOL STUDIES

4.1 Cloud microphysical study: August 14, 2004

On the 14th of August, northwesterly flow was helping to initiate storms over northeastern New Mexico within a region of upslope and moisture convergence. Activity extended southeastward along an instability axis to just west of Amarillo Texas by 2330 UTC. Instability was varied across the region with models indicating an axis of 1000 J/kg of boundary layer CAPE extending northwestward from Big Spring Texas to northeastern New Mexico. The airmass could be typified as a modified continental air mass with trajectories coming increasingly off the Gulf of Mexico. Cloud base temperatures based upon model soundings were expected to be around 13°C to 15°C. The 0000 UTC Amarillo sounding, most representative of the sampled environment indicated CAPE values of 652 J/kg.

Aircraft penetrations were made on the flanks of a severe thunderstorm that developed in Deaf Smith county west of Amarillo. The cloud bases formed along an incline as they developed over a gust front close to the thunderstorm. To the west of the thunderstorm (about 10 miles from the intense aircraft radar echo) the cloud bases were firm at 7100 feet. Further west, the cloud bases were higher by about 1000 feet. Apparently aircraft penetrations were conducted on clouds that were triggered by the gust front to the southwest of the thunderstorm. The clouds had no discernible updraft on the aircraft Vertical Speed Indicator (VSI) at their bases, but they became quite violent higher up. The cloud was pushing erected towers against the apparent strong shear towards the parent storm that was visible in the more mature towers. New growth was apparent on the northwest and the southwest flank of the storm. This thunderstorm produced hail that was larger than 2 inches in diameter.

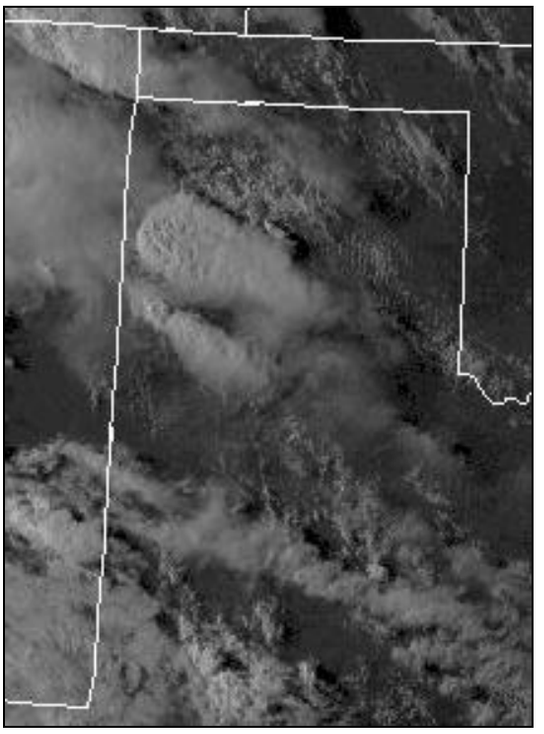

Figure 3: Visible Image 14 Aug 04 23:32Z

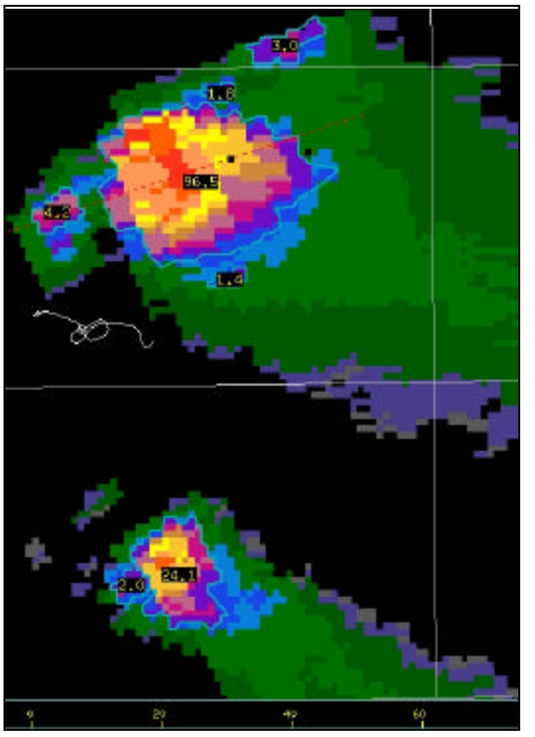

Figure 4: NEXRAD radar image as viewed on TITAN 14 Aug 04 23:28Z with the research aircraft track on the southwest flank of the northernmost thunderstorm.

Cloud penetrations were made in the same cloud and each aircraft maneuver to reverse course to the cloud was a procedure turn. The present analysis will focus on measurements made on a convective tower building along the gust front. Eleven aircraft penetrations were made in 26 minutes on the southwest flank of the mature thunderstorm (Figure 4) from the cloud formation level at an altitude of 7100 feet (2200 m) to around 21000 feet (6500 m). Table 2 lists the general characteristics of this cloud.

Cloud liquid water content as large as 1.9 gm^{-3} (CDP calculated) was observed in this cloud. The values of liquid water content from the hotwire Liquid Water Content (LWC) sensor were within 15% of adiabatic values, but near the cloud top hotwire LWC values were about 40% of the adiabatic values.

The Cloud Droplet Probe (CDP) concentration increases above the cloud base, with maximum observed cloud droplet concentrations at 1950 cm^{-3} around 3400 feet above the cloud formation level. The droplet concentrations decrease to 575 cm^{-3} at the cloud top.

In general, peak CDP concentrations occur when the aircraft encounters upward moving air close to the cloud base, but this relationship loses its trend towards the cloud top as the cloud drafts become more vigorous. The CDP Effective Diameter (Deff) remains relatively constant during each penetration indicating that the cloud drafts are not necessarily affecting the cloud droplet diameters. However, the largest LWC were co-located with the strongest updrafts especially from the cloud base through the mid levels.

Regions with low LWC generally correspond to reduced cloud droplet concentrations and weak cloud drafts or downdrafts. This trend can be observed in both the CDP calculated LWC and the hotwire LWC. An exception to this latter observation is penetrations at the cloud top where distributions in the vertical velocity are much wider and more turbulent. At the cloud top, the trend in the CDP concentration followed the trend in the Cloud Imaging Probe (CIP) concentrations very closely. The CDP spectra at the cloud base were generally narrow (Figure 5) becoming more flat and wide at the mid levels and the cloud top (Figure 6). Figures 7, 8, 9 and 10 summarize the vertical profile of the cloud hydrometeor distributions and the cloud drafts.

GPS altitude (m)	Penetration time (s)	Vertical velocity (+ Down) (ms^{-1})	Hotwire LWC, adiabatic LWC (gm^{-3})	Max CDP conc (cm^{-3})	Max CDP Deff, Mean CDP Deff (μm)	Max CIP conc (cm^{-3})	Max CIP Deff, Mean CIP Deff (μm)
2518 to 2536	34	-3.8 to 2.5	0.23, 0.2	1361	12.4, 10.3		
2626 to 2855	49	-2.2 to 4.9	0.26, 0.3	1438	12.6, 10.4	10	38.7
3313 to 3423	55	-6.9 to 7.1	0.6, 0.6	1950	14.5, 11.8	21	36.9
4036 to 4229	57	-6.5 to 9.8	0.7, 0.8	1148	15.6, 12.2	321	358.2, 40.0
4671 to 4929	57	-15.3 to 5.8	1.1, 1.2	1206	17.3, 15.3	862	679.6, 147.5
5421 to 5645	24	-15.7 to 36.2	1.4, 1.4	1066	18.8, 18.0	2472	659.1, 442.5
6081 to 6179	26	-17.0 to 9.4	1.1, 1.6	783	18.9, 17.0	3102	659.0, 357.8
6236 to 6444	40	-4.0 to 13.7	1.0, 1.7	575	19.2, 17.0	3201	761.7, 438.1

Table 2: Summary of cloud characteristics for penetrations conducted on the 14th August 2004.

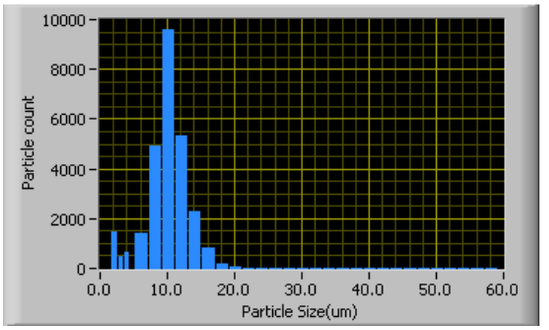

Figure 5: Narrow DSD just above the cloud formation level at around 2500 m.

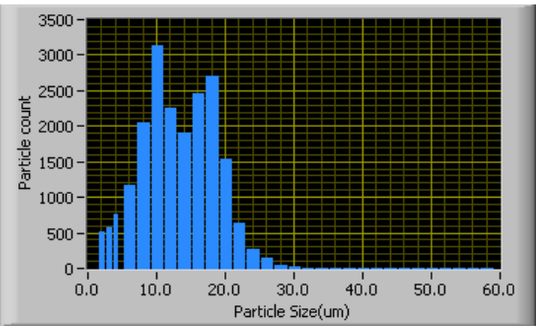

Figure 6: Wide and flat DSD at around 5500 m.

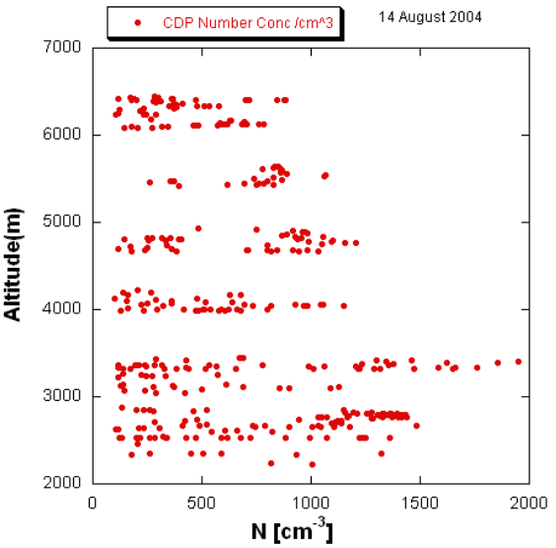

Figure 7: CDP number concentration (N) as a function of height.

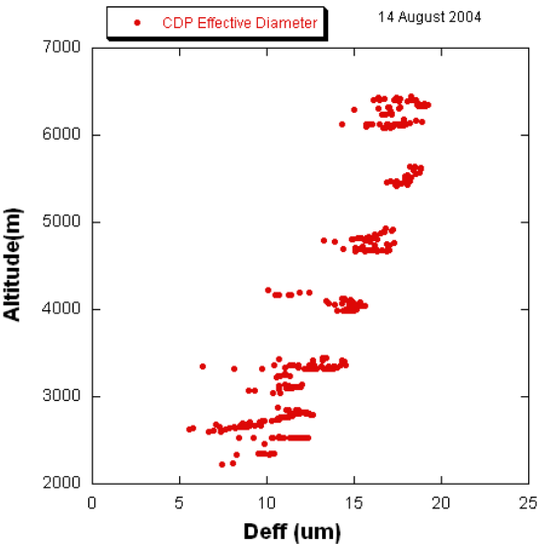

Figure 8: CDP Effective diameter (Deff) as a function of height.

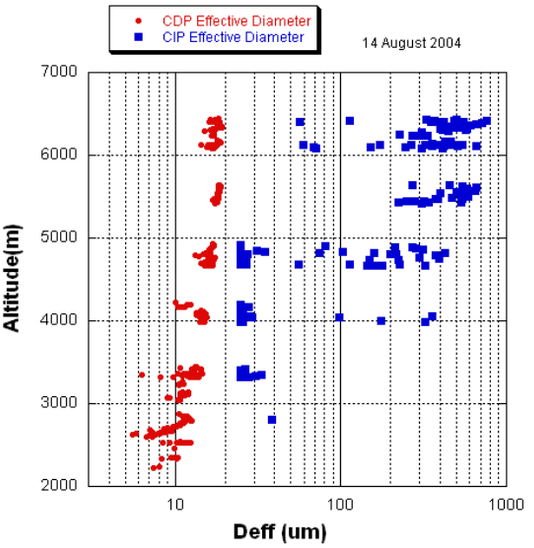

Figure 9: CDP and CIP Effective diameter (Deff) as a function of height.

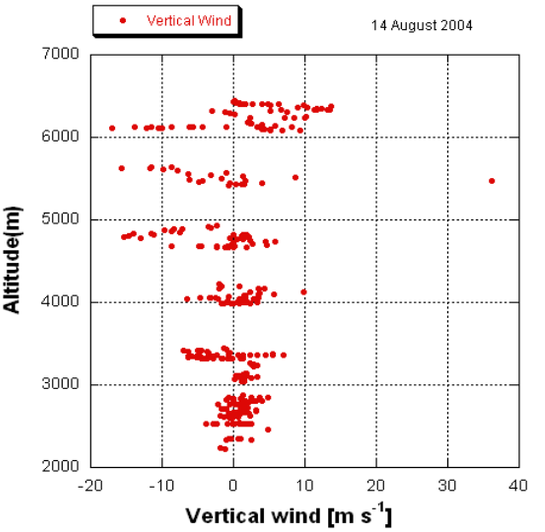

Figure 10: Vertical wind as a function of height (positive is a downdraft).

The cloud droplet concentrations are relatively high throughout the vertical profile with cloud droplet effective diameters varying from around 6 to 19 µm. These cloud droplets are small and do not increase much with height. This indicates that both the warm phase and mixed phase precipitation are very inefficient. The CIP shows that precipitation size droplets are measured mostly above 4.6 km indicating the initiation of precipitation. Cloud drafts appear to increase in intensity with height in the cloud. The highest downdraft was recorded at 5.5 km at 36.2 ms^{-1}. This was followed by a strong updraft of 15.7 ms^{-1} eleven seconds later into the penetration.

4.2 Aerosol study: August 23, 2004

Deep southerly flow had become entrenched across south central Texas with very moist low level air in place across the region. Backward trajectories from Houston indicated low-level air originating from the central Gulf of Mexico. The airmass was moderately to highly unstable as the 12Z Lake Charles, Louisiana sounding indicated a CAPE value of 1867 J/kg with only 11.6 J/kg of CIN. During the morning hours, a complex of thunderstorms was located southwest of San Antonio with the anvil spreading across much of the southern Texas coast. On the morning of August 23, the SOAR research aircraft was launched from College Station to investigate CCN and aerosol concentrations within the Houston area. Meteorological conditions in College Station were isolated thunderstorms with a southerly wind, scattered clouds at 1200 feet and broken at 3600 feet. Conditions in Houston were similar with isolated showers north of Houston and cumulus south of Houston. The aircraft flew below doud base along a west northwest -east southeast grid north of downtown Houston followed by three legs just west of the Houston ship channel.

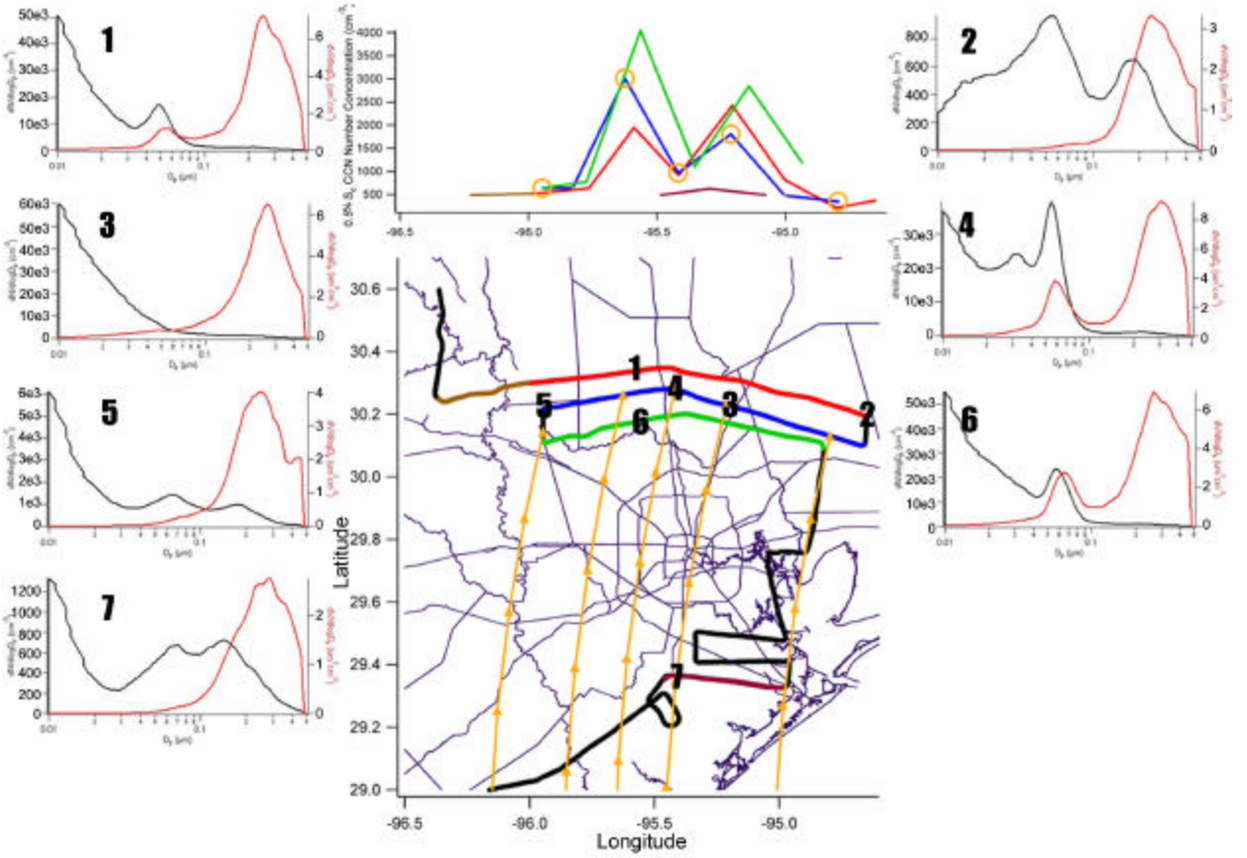

Figure 11: Data collected by the SOAR Cheyenne II during a flight downwind and upwind of Houston. Calculated backtrajectories are represented by the five yellow lines that terminate along the blue leg of the flight track. The line colors used in the top graph showing measured CCN concentration at 0.5% reflect the position along the flight track shown on the map. CCN concentrations immediately downwind of Houston were observed to be as much as 10 times higher than that measured on the east, west, and south sides of the urban plume. The cause of the bimodality in concentration is not known, although similar observations were made during the TexAQS study in 2000. Aerosol size distributions are shown in the seven numbered graphs. The position of the aircraft during each of these measurements is identified by the corresponding numbers along the flight track. Both number (black trace) and volume (red trace) distributions are shown in each graph. Total aerosol concentration was substantially greater within the Houston plume than outside of it, while total aerosol volume concentration differed by only about a factor of two.

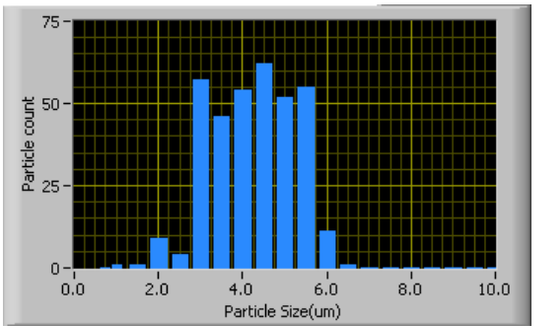

Figure 12: CCN size distributions generally flat from 2 to 6 μm away from the urban plume. CCN number concentration of 565 cm^{-3} at 0.25% supersaturation.

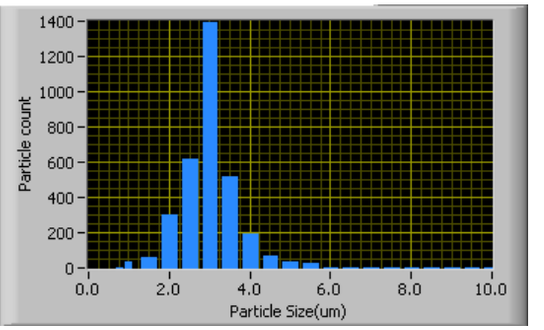

Figure 13: CCN size distributions in the urban plume with a mode around 3 μm. CCN number concentration of 4566 cm^{-3} at 0.25% supersaturation.

Background CCN concentrations were on the order of 200 to 600 cm^{-3} at 0.25% supersaturation and 400 to 800 cm^{-3} at 0.5% supersaturation. The CCN size distribution was typically broad with a mean diameter around 4μm (Figure 12). When the aircraft approached location 1, the CCN concentration increased to around 4000 cm^{-3} with peaks reaching 10000 cm^{-3}, indicating that the measurements were being made in the urban pollution plume. At this point, the CCN size distributions were typically narrower with a mean diameter around 3μm (Figure 13). An interesting feature of these measurements is that two distinct peaks in CCN concentration are apparent (Figure 11). Brock et al. (2003) noted a similar structure in their measurements, and attributed the left most peak to the emissions from a coal-fired power plant.

The DMA/TDMA system made measurements of the aerosol size distribution from 0.010μm to 0.500 μm. These measurements indicate a very dramatic increase in aerosol concentration that coincides with the increase in CCN concentration. The effect of Houston on aerosol number concentration and size distribution can be clearly seen along the streamline intersecting points 3 and 7 in Figure 11. The dramatic increase in number concentration between measurements at point 3, upwind of Houston, and point 7, downwind of Houston, indicates that large numbers of small particles were added to the air mass as it passed over the Houston area. The change in volume concentration between these points is much less pronounced. This suggests that Houston emissions may have a significant impact on CCN concentrations even when mass concentration measurements, which are more sensitive to larger particles, are largely unaffected.

5. SPECTRA's VISION

After significant administrative delays, the Texas, southeastern New Mexico and Oklahoma weather modification research effort under SPECTRA got started. Phase 1, focusing on the documentation of CCN number concentrations and size distributions and their impacts on the DSDs of clouds ingesting them, has been completed as planned. Upon analysis, the CCN climatology and resulting drop size distributions will be important to understanding cloud processes throughout Texas, especially under deliberate and inadvertent (urban pollution) seeding. Although Phase 2, involving the observational documentation of seeding signatures, has been postponed until spring 2005, the effort has already produced intriguing evidence for a strong seeding signature following hygroscopic salt-powder seeding at cloud base as described by Woodley et al. (2005) in the companion to this paper.

SPECTRA is aimed at developing scientifically proven cloud seeding technologies for precipitation augmentation in Texas, southeastern New Mexico and Oklahoma. “Proven” is to be interpreted in terms of the “proof of concept” criteria set forth by Silverman (2001;2003) involving physical and statistical evidence for seeding effects. According to Silverman (2003), the statistical evidence for rain enhancement by cloud seeding is strongest for hygroscopic seeding. Even then, he makes a cogent argument that the physical evidence for effects of hygroscopic seeding is lacking in some areas, especially as it relates to the conceptual models that have guided randomized hygroscopic seeding experimentation.

The SOAR effort and the SPECTRA program have been designed and implemented with these deficiencies in mind. SPECTRA's first priority is at narrowing the gaps in the physics of hygroscopic seeding, and it has done a significant first step towards that goal in Woodley et al. (2005). The plan aims for using the state-of-the-art tools to document the role of natural and anthropogenic (pollution) aerosols on clouds and precipitation in Texas and the effects of deliberate glaciogenic and/or hygroscopic seeding on cloud processes.

Acknowledgments. This research was supported by the Weather Damage Modification Program administered under the Bureau of Reclamation (BOR), U.S. Department of interior, Interagency Agreement No. 03-FC-81-0890. The authors gratefully thank George

Bomar from the Texas Department of Licensing and Regulation for administering the BOR grant agreement, Gary Walker (SOAR) for piloting the research aircraft, Caleb Midgley (SOAR) for his weather forecasting support and Ronen Lahav from the Hebrew University of Jerusalem for his assistance in the field program. The first author gratefully acknowledges the field support of all the Texas weather modification Program Meteorologists, including Stephanie Beall, Todd Flanagan, Ray Jones, Christine Lopez, Orlando Nunez, Archie Ruiz, and James Salesky.

REFERENCES

Brock, C. A., et al., 2003: Particle growth in urban and industrial plumes in Texas. *J. Geophys. Res.*, 108, doi:10.1029/2002JD002746.

Gasparini, R., R. Li, and D. R. Collins, 2004: Integration of size distributions and size-resolved hygroscopicity measured during the Houston Supersite for compositional categorization of the aerosol. *Atmospheric Environment*, **38**, 3285-3303.

Silverman, B. A. 2001: A Critical Assessment of Glaciogenic Seeding of Convective Clouds for Rainfall Enhancement. *Bull. Amer. Meteor. Soc.*, **82**, 903–924.

Silverman, B. A., 2003: A critical assessment of hygroscopic seeding of convective clouds for rainfall enhancement, Bull. Amer. Meteor. Soc., 84, 1219-1230.

Woodley, W. L., D. Rosenfeld, D. Axisa, R. Lahav and G. Bomar, 2005: On the Documentation of Microphysical Signatures Following the Base-Seeding of Vigorous Texas Clouds Using Glaciogenic and Hygroscopic Agents. 16th Conference on Planned and Inadvertent Weather Modification.